

Viscoelastic modeling with simultaneous microseismic sources

Shengwen Jin and Fan Jiang, Halliburton-Landmark; Xianhuai Zhu, ConocoPhillips

Summary

Various seismic sources including pressure source, vertical source, radial source, transverse source and explosive source have been widely used in exploration seismology. Double couple (DC) source and sources defined by general moment tensor are commonly used for simulation of earthquake and microseismic waves. Processing of the recorded data helps reconstruct the subsurface image and locate the microseismic events for better understanding and interpreting the geologic structures and formations. Individual sources excited at different times will form simultaneous sources. Implementation of simultaneous sources provide flexibility in survey geometries and increase spatial sampling via increased source sampling and vector-offset sampling (Hampson, et al., 2008). In this abstract, we describe the physical mechanisms of several typical seismic and microseismic sources and their impact on the synthetic wavefield. Microseismic modeling in viscoelastic media is discussed by using simultaneous sources with different source characteristics. Through the back propagation of the recorded data, the location of microseismic events can be imaged without picking the events.

Introduction

Seismic exploration has long been an important part of hydrocarbon drilling and production processes. Various seismic sources have been used in the field, such as dynamite, thumper trucks and air guns. Acquisition of seismic wavefields can be performed using geophones, hydrophones, and the like. Processing the acquired seismic data helps better understand and interpret the geologic structures and formations.

Microseismic monitoring is the placement of receiver systems from which small earthquakes induced by hydraulic fracturing can be detected and located to provide geometric and behavioral information (Zhu et al., 1996; Warpinski, 2009; Maxwell et al., 2010). To monitor hydraulic fractures and understand the seismic responses associated with subsurface material, synthetic data is usually generated from seismic modeling for validating field seismic data and monitoring fluid process at the reservoir scale (Warpinski, 2005; Brzak et al., 2009). A multiple seismic source mechanism is proposed to simulate a synthetic seismic data that models the often-complex signals received in actual microseism exploration. The ability to simulate the impact of multiple types of seismic sources provides additional insight into the study of geologic structures and reservoir characterization.

The physical mechanism of several types of seismic and microseismic sources is described in detail and illustrated in this abstract. Impact of the different source radiation pattern is clearly demonstrated on the wavefield snapshots and seismograms. Multiple sources with different characteristics are excited at different locations in different times for simulation of microseismic events. The analysis of amplitude spectrum in viscoelastic media indicates that wave amplitude will decrease with quality factor decreases for any single source or multiple simultaneous sources. Several tests with different quality factors indicate that the decreasing rate of wave amplitude is not linearly proportional to the decrease of quality factor. The relation tends to be exponential. Back propagation of the recorded data is used for locating the microseismic events.

Excitation of seismic source

Seismic exploration uses viscoelastic forward modeling to simulate wave motion in real media and extract subsurface information. The nature of the source event of viscoelastic forward modeling may be described as a system below. This system integrates all types of source mechanisms which are regularly performed for monitoring hydraulic fracture and validating seismic data for subsurface imaging and illumination. The excitation system of seismic sources involved in the modeling procedure can be characterized in the followings:

1. Pressure source: a stress-rate source applied to stress component which only generates P-wave.
2. Vertical source: a body force source applied to vertical component (z) of particle velocity which generates both P-wave and S-wave.
3. Radial source: a body force source applied to radial component (x) of particle velocity.
4. Transverse source: a body force source applied to transverse component (y) of particle velocity. Radial and transverse source can generate both P-wave and S-waves.
5. Vector source: a body force source designed for simulating microseism mechanism. Vector source is performed on all three components (x, y and z) of particle velocity with directional coefficients of each component.
6. DC source: a shear dislocation source representing earthquake source. DC source specifies the source radiation pattern and can be described as an equivalent distribution of body force source. As shown in Figure 1, four fault parameters, i.e., source magnitude, strike angle (φ), dip angle (δ) and rake angle (λ), are

Viscoelastic Modeling with Simultaneous Microseismic Source

introduced to describe the DC source mechanism (Aki and Richards, 2002).

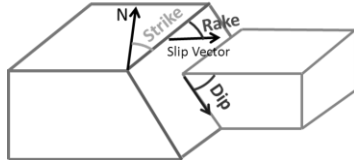


Figure 1: Description of fault parameters.

7. Moment tensor source: a generalized source that represents the response of a fault of any arbitrary orientation. It is formed as a 3x3 matrix with normalization to unit amplitude:

$$M = m_0 \begin{bmatrix} m_{11} & m_{12} & m_{13} \\ m_{21} & m_{22} & m_{23} \\ m_{31} & m_{32} & m_{33} \end{bmatrix} \quad (1)$$

where m_0 is the seismic moment and $m_{ij}(i, j = 1, 2, 3)$ represents a force couple. The generalized moment tensor source is described as a distribution of body forces that added to the individual component of particle velocity component (Grave, 1996). DC source is a special case of moment tensor sources.

Index	Moment Tensor	DC Parameter	Radiation Pattern	Snapshot (z)	Gather (z)
1	$\begin{bmatrix} 1 & 0 & 0 \\ 0 & -1 & 0 \\ 0 & 0 & 0 \end{bmatrix}$	$\varphi = 45^\circ$ $\delta = 90^\circ$ $\lambda = 180^\circ$			
2	$\begin{bmatrix} 0 & 0 & 1 \\ 0 & 0 & 0 \\ 1 & 0 & 0 \end{bmatrix}$	$\varphi = 270^\circ$ $\delta = 90^\circ$ $\lambda = 270^\circ$			
3	$\begin{bmatrix} -1 & 0 & 0 \\ 0 & 0 & 0 \\ 0 & 0 & 1 \end{bmatrix}$	$\varphi = 90^\circ$ $\delta = 45^\circ$ $\lambda = 90^\circ$			

Figure 2: Characteristic comparison of three different seismic moment tensor sources with $V_p=2.0$ km/s, $V_s=1.0$ km/s, maximum frequency is 40 Hz. All snapshots and shot gather traces are extracted from vertical particle velocity component. The shot gather trace is picked from offset at 0.4 km.

Viscoelastic modeling of simultaneous microseismic sources

Seismic viscoelastic modeling typically performs simulation based on the propagation of simulated seismic waves generated by a single type of seismic source. In real world seismic exploration, multiple types of seismic

sources may be present at a given time. Particular location, size and orientation are parameters to determine pre-existing natural fracture network. Multiple simultaneous source information could be used to gain the input parameters and define stress orientations, and verify the direction of fracture movements.

Carcione (1993) investigated attenuation in viscoelastic media and developed the corresponding stress-velocity wave equations, where memory variables are introduced to model the relaxation mechanism. Attenuation effect is represented by quality factor Q defined as:

$$Q = \frac{\text{Energy of seismic wave}}{\text{Energy dissipated per cycle of wave}} \quad (2)$$

The relation between quality factor Q_p (for P-wave), Q_s (for S-wave) and the relaxation time in standard linear viscoelastic equations is described as (Blanch et al., 1995):

$$\tau_\sigma = \frac{1}{\omega} \left(\sqrt{1 + \frac{1}{Q_p^2}} - \frac{1}{Q_p} \right) \quad (3a)$$

$$\tau_\varepsilon^P = \frac{1}{\omega^2 \tau_\sigma} \quad (3b)$$

$$\tau_\varepsilon^S = \frac{1 + \omega \tau_\sigma Q_s}{\omega Q_s - \omega^2 \tau_\sigma} \quad (3c)$$

Here τ_σ and τ_ε are the relaxation times for P- and S- wave, ω is frequency. Here Equation 3 describes a group of relaxation times for single relaxation mechanism in a standard linear solid.

Figure 3a shows a snapshot of simultaneous source system in a constant velocity model. In this example P-wave velocity is 2.0 km/s, S-wave velocity is 1.0 km/s and density is 2.0 kg/m³. The quality factor for Q_p and Q_s are identical and equal to 20. Ricker wavelet is used with maximum frequency 30 Hz. Three moment tensor sources (located at 1.0 km below surface) are introduced with delayed excitation time 0.0 s, 0.2 s, 0.4 s respectively. By implementing multiple source system with viscoelastic modeling, it is possible to extract source parameters from the seismic events and understand the information such as fault dimension and seismic moment when comparing with field microseismic data. Figure 3b and 3c show that shot gathers of elastic and viscoelastic modeling of the recorded vertical component data at surface receivers. Eaton (2009) described a least-square solution to find best resolved components of moment tensor from direct arrival between data and model. However, cross talks of multiple sources may bring more complex features and coherent noises.

Viscoelastic Modeling with Simultaneous Microseismic Source

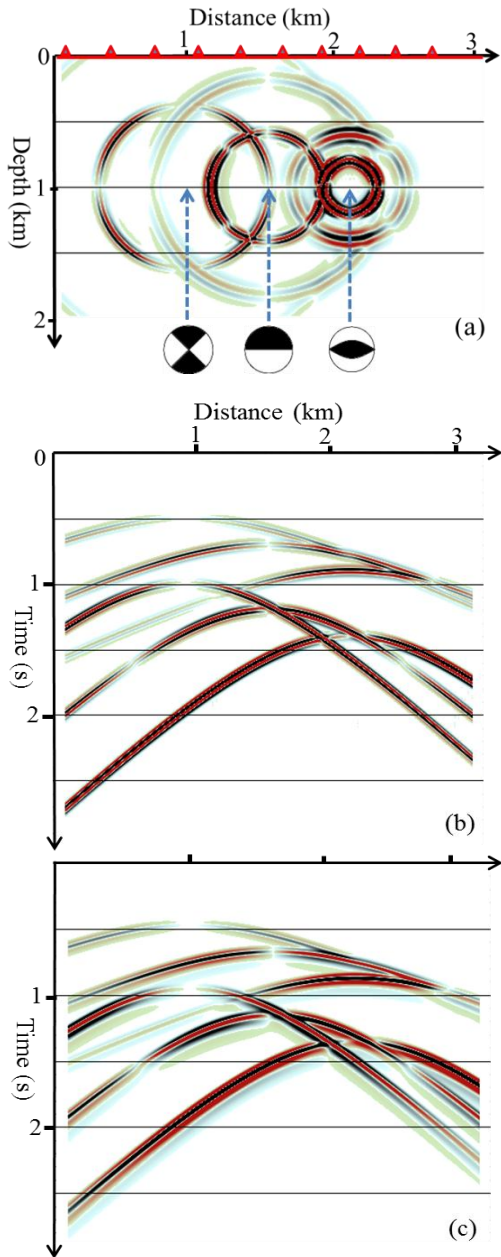


Figure 3: (a) Snapshot of viscoelastic wave propagation at $t=0.6s$. (b) Elastic shot gather with simultaneous microseismic sources (c) Viscoelastic shot gather with simultaneous microseismic sources. Viscoelastic shot gather shows lower frequency band compared with elastic gather. Red triangles are surface receivers. (Are they vertical component?)

Figure 4 describes the distribution of amplitude over frequency between different quality factors on viscoelastic modeling. Figure 4a shows that amplitude distribution at different frequencies with only one microseismic source (source index 1 in Figure 2). Figure 4b shows that the amplitude distribution with simultaneous sources (shown in Figure 3a). Introducing quality factor to wave simulation will absorb energy and lower the frequency band. This phenomenon not only appears on single microseismic source, but also takes effect on simultaneous microseismic sources. Several tests on point-source excitation also obtain same result.

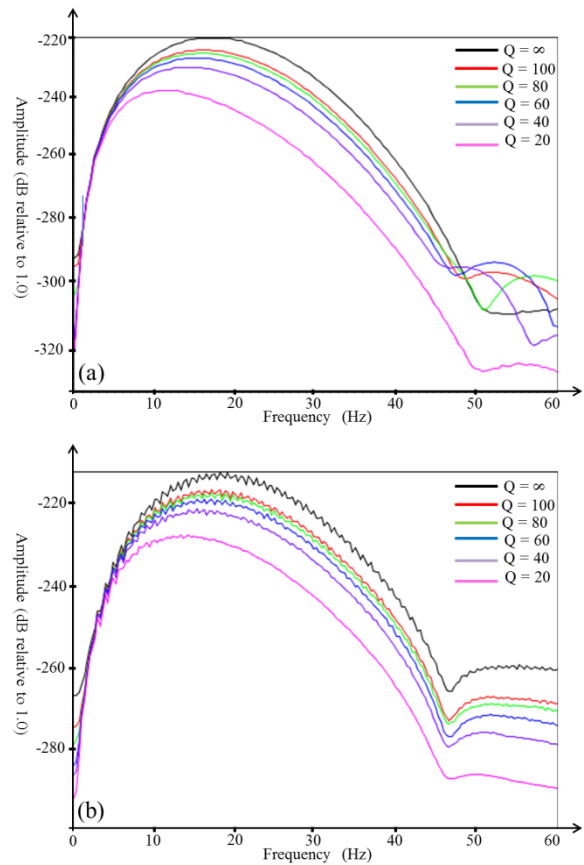


Figure 4: Distribution of amplitude at different frequencies on (a) a single microseismic source and (b) simultaneous sources. Quality factor Q ($Q_p = Q_s$) is range from infinite (elastic case) to 20.

We further analyse the relation between amplitude and quality factor with excitation of simultaneous sources. Figure 5 shows that the loss rate of amplitude is not linearly proportional to variation of quality factor. We use loss rate to quantify the variation of amplitude versus quality factor.

Viscoelastic Modeling with Simultaneous Microseismic Source

Here the loss rate is defined as $(1 - A_{max}(\text{viscoelastic}) / A_{max}(\text{elastic})) * 100$ with different quality factors. A_{max} stands for maximum amplitude. When maximum frequency of source wavelet is 30 Hz, the loss rate of viscoelastic wave with $Q = 100$ is 40%, which means around 60% wave energy dissipated due to attenuation. When $Q = 60$, the loss rate slowly increases to 50%. However, when $Q = 20$, the loss rate dramatically increases to over 85%. This may help us on explanation and estimation of intrinsic amplitude change due to attenuation on simultaneous sources.

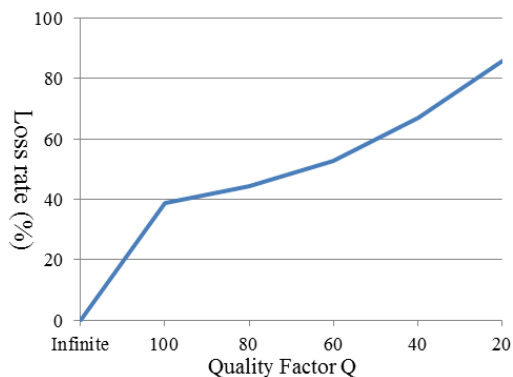


Figure 5: The loss rate of amplitude versus different quality factors on excitation of simultaneous sources.

Back propagation of the recorded microseismic data with simultaneous sources is used for locating the multiple microseismic events. Figure 6 shows an example of imaging simultaneous microseismic events. The back propagated wavefield interferes constructively at the three source positions at different times. Over- or under-migrated events cause unfocused energy. Some artifacts are present on the image. Further study needs to be conducted to get a clean and high resolution image.

Conclusions

Seismic source, which generates controlled seismic energy, is used to perform reflection, refraction and passive seismic surveys. In this abstract, we describe physical mechanisms of several popular seismic and microseismic sources. Different radiation patterns show different impacts on wavefield snapshot and seismogram. We discussed with a simultaneous source system which could use in arbitrary acquisition geometry for different purposes. Applying simultaneous sources to viscoelastic modeling provides capability of understanding the source and fracture mechanisms, especially for microseismic data. Our test shows that the attenuation has a significant effect on seismograms. Wave amplitude will have greater loss rate when quality factor is less than 50 and frequency will shift to lower band. Test of back propagation with simultaneous

sources shows that the recorded data could be used to locate microseismic events without picking for multiple source application. The imaged source locations and source mechanisms can help interpretation of the wave modes and behaviors of hydraulic fractures.

Acknowledgements

We thank Mike Davidson, Wenjie Jiao, Joel Brewer and Chuck Mosher of ConocoPhillips and Yiqing Ren of Landmark for constructive discussions. We also thank Halliburton and ConocoPhillips for permission to publish the results.

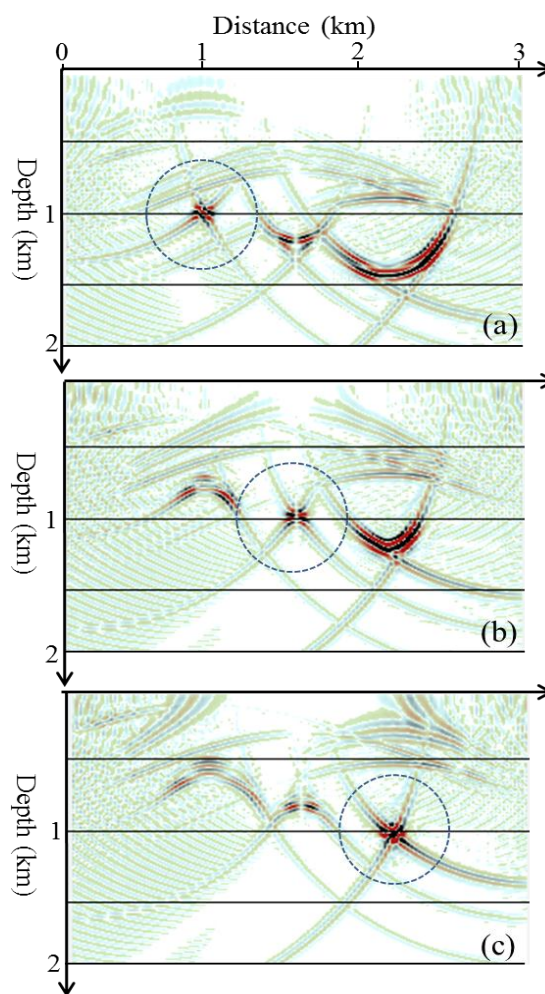


Figure 6: Imaging result of simultaneous microseismic events (dashed circles) via back propagation at (a) 0.0s, (b) 0.2s, (c) 0.4s delayed excitation time. True locations for three sources are at 1.0 km below surface.

<http://dx.doi.org/10.1190/segam2013-0223.1>

EDITED REFERENCES

Note: This reference list is a copy-edited version of the reference list submitted by the author. Reference lists for the 2013 SEG Technical Program Expanded Abstracts have been copy edited so that references provided with the online metadata for each paper will achieve a high degree of linking to cited sources that appear on the Web.

REFERENCES

- Aki, K., and P. G. Richards, 2002, Quantitative seismology, second edition: University Science Books.
- Blanch, J. O., J. O. A. Robertsson, and W. W. Symes, 1995, Modeling of a constant Q: methodology and algorithm for an efficient and optimally inexpensive viscoelastic technique: *Geophysics*, **60**, 176–184, <http://dx.doi.org/10.1190/1.1443744>.
- Brzak, K., Y. J. Gu, A. Ökeler, M. Steckler, and A. Lerner-Lam, 2009, Migration imaging and forward modelling of microseismic noise sources near southern Italy: *Geochemistry Geophysics Geosystems*, **10**, Q01012, <http://dx.doi.org/10.1029/2008GC002234>.
- Carcione, J. M., 1993, Seismic modeling in viscoelastic media: *Geophysics*, **58**, 110–120, <http://dx.doi.org/10.1190/1.1443340>.
- Eaton, D. W., 2009, Resolution of microseismic moment tensors: A synthetic modeling study: 79th Annual International Meeting, SEG, Expanded Abstracts, 3569–3573, <http://dx.doi.org/10.1190/1.3255606>.
- Graves, R. W., 1996, Simulating seismic wave propagation in 3D elastic media using staggered-grid finite differences: *Bulletin of the Seismological Society of America*, **86**, 1091–1106.
- Hampson, G., J. Stefani, and F. Herkenhoff, 2008, Acquisition using simultaneous sources: *The Leading Edge*, **27**, 918–923, <http://dx.doi.org/10.1190/1.2954034>.
- Maxwell, S. C., J. Rutledge, R. Jones, and M. Fehler, 2010, Petroleum reservoir characterization using downhole microseismic monitoring: *Geophysics*, **75**, no. 5, A129–A137, <http://dx.doi.org/10.1190/1.3477966>.
- Warpinski, N. R., R. B. Sullivan, J. Uhl, C. Waltman, and S. Machoyoe, 2005, Improved microseismic fracture mapping using perforation timing measurements for velocity calibration: *Society of Petroleum Engineers Journal*, **10**, 14–23.
- Warpinski, N. R., 2009, Microseismic monitoring: Inside and out: *Journal of Petroleum Technology*, **61**, 80–85, <http://dx.doi.org/10.2118/118537-MS>.
- Zhu, X., J. Gibson, N. Ravindran, R. Zinno, and D. Sixta, 1996, Seismic imaging of hydraulic fractures in Carthage tight sands: A pilot study: *The Leading Edge*, **3**, 218–224, <http://dx.doi.org/10.1190/1.1437302>.